Simon Herter * and Sarah C. L. Fischer

Fully automated calibration of an eddy current sensor for high-precision feedback in pick-and-place applications using bioinspired dry adhesives

Vollautomatische Kalibrierung eines Wirbelstromsensors für hochpräzises Feedback bei Pick-and-Place-Anwendungen unter Verwendung bioinspirierter Roboterendeffektoren

https://doi.org/10.1515/teme-2025-0067

Abstract: The integration of sensor systems in industrial applications requires not only simple technical implementation, but also an automated and scalable calibration methodology. This is a central prerequisite for reliable and easy use in adaptive robotic processes. In the present work, a systematic and fully automated process for the calibration of eddy current-based sensors is developed to enable the precise detection of misalignments in pick-and-place tasks using bioinspired robot end effectors.

For this purpose, a method for automated optical reference alignment in combination with automated data acquisition for sensor calibration was designed and implemented. The developed setup enables efficient, reproducible, and automated calibration without manual intervention. The experimental validation proves the practical suitability of the approach and underlines its potential.

Keywords: Sensor development; eddy currents; bioinspired adhesive gripping systems; robotics

Zusammenfassung: Die Integration von Sensoren in industrielle Anwendungen erfordert nicht nur eine einfache technische Implementierung, sondern insbesondere auch eine automatisierte und skalierbare Kalibrierungsmethodik. Dies ist eine zentrale Voraussetzung für den zuverlässigen und einfachen Einsatz in adaptiven Roboterprozessen. In der vorliegenden Arbeit wird ein systematischer und vollständig automatisierter Prozess zur Kalibrierung wirbelstrombasierter Sensoren entwickelt, um die präzise Detektion von Ausrichtungsfehlern bei Pick-and-Place-Aufgaben mit-

*Corresponding author: Simon Herter , Fraunhofer Institute for Nondestructive Testing IZFP, 66123 Saarbruecken, Germany, E-Mail: simon.herter@izfp.fraunhofer.de 00009-0009-8270-3861 Sarah C. L. Fischer, Fraunhofer Institute for Nondestructive Testing IZFP, 66123 Saarbruecken, Germany, E-Mail: sarah.fischer@izfp.fraunhofer.de 00000-0003-1569-276X

tels bioinspirierten Roboterendeffektoren, zu ermöglichen. Zu diesem Zweck wurde ein Verfahren zur automatisierten optischen Referenzausrichtung in Verbindung mit einer automatisierten Datenerfassung für die Kalibrierung der Sensorik konzipiert und umgesetzt. Das entwickelte Setup ermöglicht eine effiziente, reproduzierbare und automatisierte Kalibrierung ohne manuellen Eingriff. Die experimentelle Validierung belegt die Praxistauglichkeit des Ansatzes und unterstreicht dessen Potenzial.

Schlagwörter: Sensorentwicklung; Wirbelstromprüfung; bioinspirierte Roboterendeffektoren; Robotik

1 Introduction

Bioinspired dry adhesives made their way into innovative gripping solutions for robotic pick-and-place tasks. These adhesive structures mimic micropatterned surfaces found in nature, such as those found in geckos [1]. Technically, these surfaces are implemented using soft polymers by imitating the fibrils (technically called pillars) and arranging them regularly on a backing layer for contact splitting and more favorable stress distribution. The advantage of these adhesive pads is that they can be used independently without an external energy source, as they are based on the physical principle of van-der-Waals interaction. They are controlled by mechanical forces, allowing them to switch between the gripping and releasing states. The magnitude of adhesive force is affected by factors such as roughness, contamination on the surface, temperature and humidity, for example. The adhesive pads are highly sensitive to alignment and positioning relative to the target surface, resulting in loss of more than 30 % of adhesion force for misalignment angles of only 0.2° as shown by Kroner et al. [1–7]. For the application of synthetic dry adhesives in pick-and-place applications, reliability and speed are of great importance in order to

integrate in automated manufacturing lines. Optimal, reliable adhesion performance can only be achieved when the adhesives are precisely aligned with the substrates, making real-time monitoring of the contact and misalignment highly desirable. To enable this, an eddy current-based sensor system was developed to detect pad alignment during pick and place tasks [8]. Such eddy current-based sensors have recently also shown to overcome limitations like contamination or external magnetic fields, from which comparable sensor concepts like magnetic or capacitive sensors suffer [9– 11]. For the use of eddy current sensors in the prediction of tilt, it is essential to calibrate the measuring coils in order to transfer the sensor data in physically interpretable quantities, allowing to compute the tilt angle during the manipulation of objects. To ensure consistent high precision under varying conditions and compensate for mechanical or environmental deviations, fully automated calibration of the sensor is necessary, so it could be a cost effective and easy to deploy sensor system. This work focuses on the development and evaluation of a fully automated setup for eddy current sensor distance calibration, designed to provide reliable feedback in pick-and-place operations using bioinspired dry adhesives.

2 Experimental Setup

In this section, the experimental setup containing the robotic system with the frustrated total internal reflection (FTIR) stage as well as the modular sensor concept modified based on [8] are presented.

2.1 Robotic setup

The experimental setup consists of a robotic arm (Meca 500) with an FTIR system for optical referencing of the adhesive pads and a load cell for force measurement (Figure 1). The developed eddy current sensor for displacement detection is attached to the robotic arm in combination with the bioinspired adhesive pads in order to mimic a setup for pick-and-place tasks.

The frustrated total internal reflection (FTIR) stage is located on the table and used for optical alignment of the microstructured surfaces. FTIR is a measurement principle which can be used to detect contact on a transparent surface. For this purpose, light is coupled into a glass plate. Initially, the different refractive indices between the air and glass interfaces result in total reflection. Where the pillars are in contact with the glass plate, the reflection conditions

change and the light can be coupled out of the glass plate. This effect is used to visualise contact surfaces of bioinspired structures. In this work, the FTIR setup is used to establish the aligned reference state of pillars and substrate, which serves as the baseline for calibration.

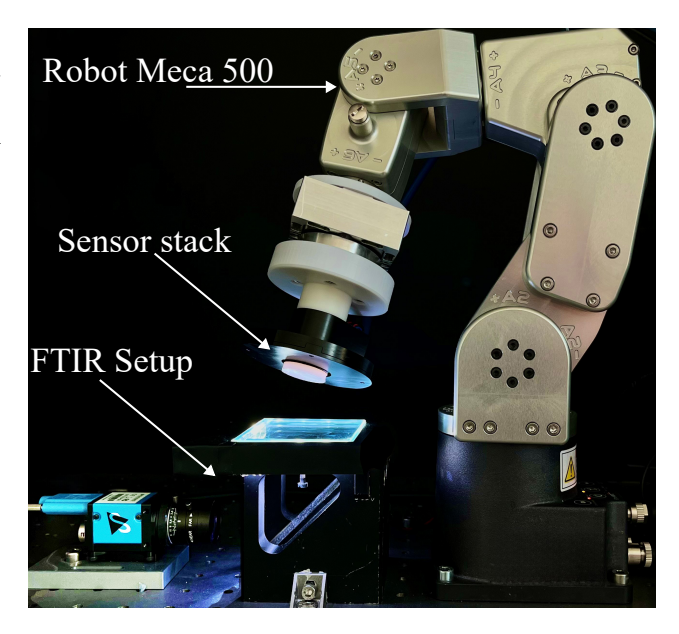


Fig. 1: Image of experimental setup for auto calibration.

2.2 Sensor design and operation

The developed sensor system follows a modular design, consisting of four primary components: (1) printed circuit board (PCB) coils, (2) a deformable layer, (3) a measurement layer, and (4) the adhesive pad. Previously, the sensor configuration comprised a single transmitting coil and three receiving coils, with calibration performed without the adhesive pad attached. In contrast, the new design (Figure 2) utilizes one transmitting coil and four receiving coils, and is calibrated as a complete assembly, including the adhesive pad. This approach accounts for potential variations due to assembly tolerances or material inconsistencies, ensuring that the sensor is calibrated in its fully operational configuration.

The sensor, with a diameter of 24 mm, utilizes multiple receiving coils to detect voltage and phase shifts generated by a transmitting coil in response to a conductive reference plane positioned behind the adhesive pad. For deployment in real-world applications, the raw voltage and phase signals extracted via IQ demodulation must be calibrated against actual displacement values to enable meaningful interpretation of angular deviations. In the scope of this analysis, only voltage variations are considered, as they represent

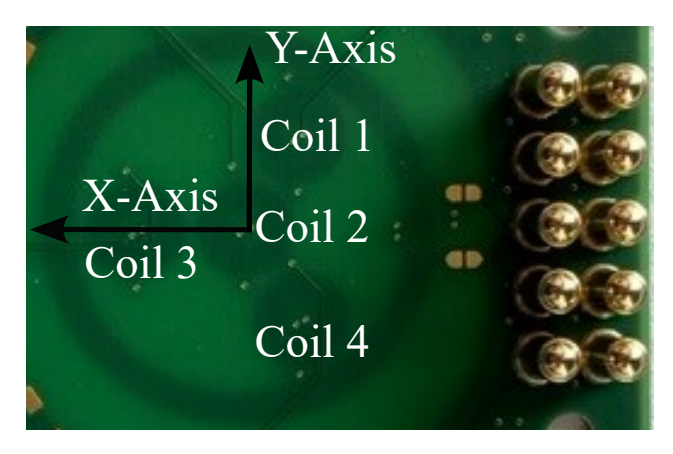


Fig. 2: Image of sensor with coordinate system and coil positions (seen through)

the primary measurable effect derived from the amplitude of the demodulated IQ signals as previously described by Herter et al. [8].

Phase information is used qualitatively to determine the direction of displacement. A positive phase sign indicates that the conductive material is approaching the transmitting coil, whereas a negative sign indicates that it is moving away. This directional sensitivity is essential for interpreting angular deviations during robotic pick-and-place operations involving soft adhesive contacts.

Furthermore, the traditional wired connection has been replaced with a modular spring-loaded ball contact, enabling a more flexible and easily interchangeable mechanical and electrical interface between the sensor system and various robotic arms. This design ensures compatibility across different robotic platforms while maintaining a consistent electrical connection.

Signal excitation and acquisition are managed by a custom-designed electronic board, as described in [8]. To enhance processing capabilities, the existing electronic setup used in prior studies has been extended with the integration of a Raspberry Pi 4. This addition significantly accelerates computational performance and facilitates seamless integration into the measurement and control framework via User Datagram Protocol (UDP) communication. As a result, the system achieves a data transmission rate of 331 s⁻¹, ensuring delivery of high-resolution, information rich sensor data to the robot control unit, thereby meeting the demands of real-time operation.

3 Proposed methodology

The methodology for automated calibration procedure includes the following steps:

- Optical alignment sequence based on FTIR
- Sensor data collection
- Calibration coefficient determination
- Validation

The automated calibration procedure involves starting several Python scripts simultaneously using the Python multiprocessing module. Each process is used individually for its respective task. For example, there is a separate process for controlling the robot, the sensor, and the camera. Data evaluation for optical alignment, signal recording, and analysis are also implemented in separate processes. The processes communicate with each other so that the above mentioned steps run consecutively.

In the following sections, the methodology of the steps will be briefly introduced before results are presented.

Step 1: Optical alignment sequence

A predefined movement sequence is initiated, during which the robotic arm moves the adhesive pad toward the glass plate incrementally by a defined distance (here 100 µm). This sequence operates in a loop until either the specified number of steps is reached (in our case 10 steps) or a defined criterion is satisfied, such as sensor signals or additional load cell data. An image is captured at each step based on the FTIR setup. The images are analyzed to evaluate the contact area by detecting circular adhesive structures using a circle Hough transformation. The center of gravity (CoG) of the detected contact pattern is calculated for each image. Over the sequence of images, the direction vector of the CoG is determined. For an ideally aligned pad, this vector remains centered at the pad's midpoint, corresponding to a value of (0, 0).

If the direction vector of the CoG shifts within 5 pixels (one pixel corresponds to approx. $32 \,\mu\text{m}$) in the X and Y directions, the pad is considered aligned. If this limit is exceeded, a correction is made based on the coordinate systems and the application of the FTIR setup corresponding to the misalignment vector until the condition is met.

Step 2: Sensor data collection

After step 1 is completed and the pad is aligned, the data collection starts by compressing the pad against the glass plate of the FTIR setup. With a step size of 100 µm, the pad is incrementally compressed and the sensor data as well as number of steps are stored channel by channel in text files for further processing. The number of steps is later

used to compute the overall displacement based on a known step size.

In this step, the mechanical properties of the adhesive pads must be considered as boundary conditions. The adhesive pads used in this study tend to buckle when the force exceeds 50 N. This buckling leads to mechanical instability within the interface between the object and the pad, resulting in a loss of adhesive force.

The procedure in step 2 is repeated 4 times. However, due to settling effects resulting in a strong hysteresis in the first loading cycle, the first measurement is not considered and the last 3 are used for evaluation.

Step 3: Calibration coefficient determination

First, calibration curves are computed to correlate signal amplitude with distance for each individual sensor coil across the 3 collected measurements from the dataset. A third-degree polynomial is then fitted to the data to model the relationship between signal amplitude and distance, as shown in [8]. To account for positive and negative signal variations, the sign is inferred from the phase angle calculated via IQ demodulation. However, near the origin of the IQ plane, where amplitude values are small (in the range of a few thousand digits), sign fluctuations may occur. To mitigate this issue, the sign is set to positive within this range to ensure calibration stability near zero displacement. This approach is valid because calibration data is only collected in the compression regime. For repeated calibration measurements, the mean of the calculated coefficients is taken for each coil. The curves are zero-centered to eliminate the need for intercepts.

Step 4: Validation

Finally, to validate the determined calibration coefficients, a validation is carried out based on the reference coordinates from step 1 to check if the alignment detection is functioning properly. Thus, the necessary level of precision can be individually defined.

4 Results and discussion

4.1 Step 1: Optical alignment sequence

Figure 3 a-d shows images of the misaligned starting sequence for increasing compression. Images in Figure 3 e-h show the reference state determined by Step 1 for increasing compression. The images show the contact points of the adhesive pad detected using the circle Hough transform, coloured in yellow and green circles, with the contact points marked in yellow indicating weaker contact, while the green

circles indicate full contact. This differentiation is based on the calculated intensity of the circles and is only for visualisation purposes but has no influence on the calculation of the CoG.

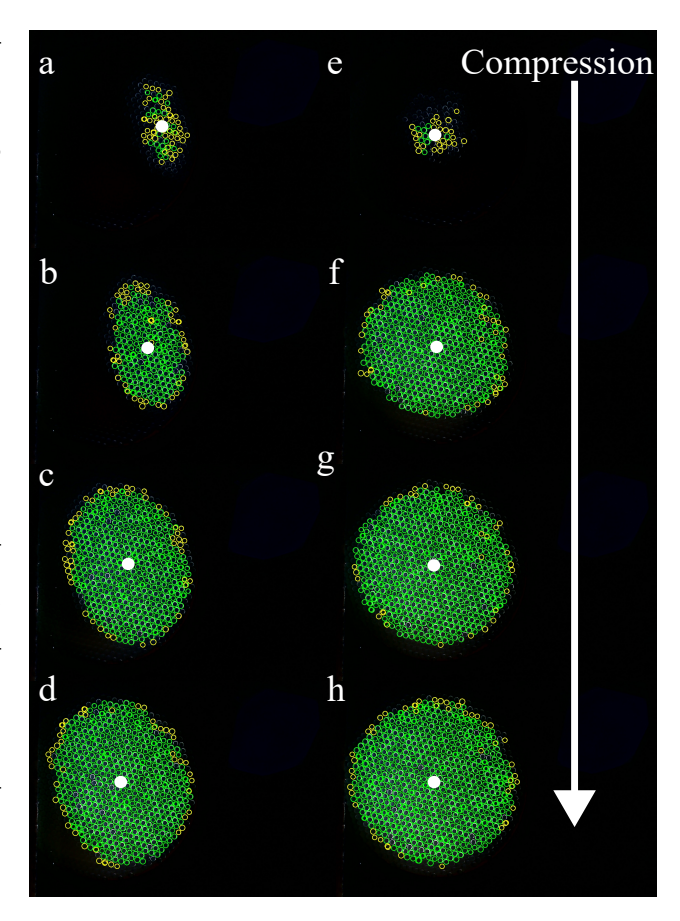


Fig. 3: Images captured during the optical alignment process. Images a-d show a sequence captured while the pad is misaligned, images e-h show the final sequence for aligned pad, pressed on glass substrate. With a white circle the CoG is highlighted for each image.

4.2 Steps 2 and 3: Sensor data collection and determination of calibration coefficient

The primary distance-to-signal curve is recorded multiple times in step 2 for each sensor coil. In order to determine the calibration factors from the sensor distance curves, it is necessary to synchronize the data using the compression distance. It is important to note that, based on this procedure, the entire sensor stack is calibrated, which means that the change in distance is not completely transferred to the deformable layer but is distributed between the individual components. For this purpose, the hysteresis curves of the deformable layer used as foam (KS865-F) and the measured displacement force curves for this system were compared. Based on the Voigt-model describing the rule of mixture for axially loaded laminar composites, the effective displacement of the measurement layer is roughly half of the displacement applied to the adhesive pad, resulting in a correction factor of 2. Note that this factor needs to be adjusted for different foam thickness, foam type and synthetic adhesive pad.

The distance-amplitude curves for the individual sensors are shown in Figure 4. The coefficients (see Table 1) are calculated for each curve and their mean values are used as calibration coefficients. Each calibration curve shows an individual correlation between distance and sensor signal, as expected based on manufacturing tolerances and system tolerances such as impedance characteristics of the coils.

Tab. 1: Calibration coefficients and corresponding standard deviations.

Coefficient	Coil 1	Coil 2	Coil 3	Coil 4
a in μm digit ⁻¹	3.29e-12	2.3e-12	9.29e-12	3.31e-12
SD a in $\mu m \mathrm{digit}^{-1}$	2.56e-13	1.61e-13	2.54e-12	6.59e-13
b in $\mu m \mathrm{digit}^{-1}$	-3.43e-7	-1.93e-7	-6.13e-7	3.41e-7
SD b in $\mu m \operatorname{digit}^{-1}$	2.07e-8	1.45e-8	1.51e-7	5.45e-8
\mathbf{c} in $\mu\mathrm{m}\mathrm{digit}^{-1}$	2.27e-2	1.8e-2	2.96e-2	2.29e-2
SD c in $\mu m \mathrm{digit}^{-1}$	4.77e-2	4.49e-2	2.7e-3	1.19e-3

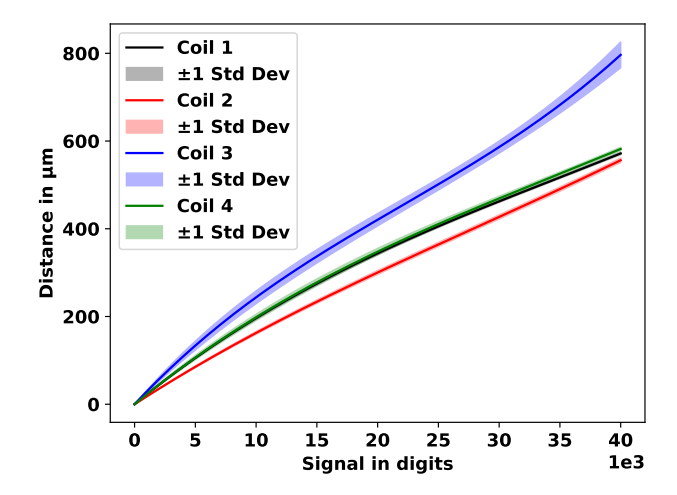


Fig. 4: Calibration curves for the 4 receiving coils.

4.3 Validation

For validation of the proposed calibration process, the sensor is tilted 0.5° and 1° along the X and Y axis (cf. 2 for axis orientation) in different experiments.

It is important to note that no reference is made to the initial angle. Instead, the absolute predicted angle is used, as it is the case in industrial applications where there is no prior knowledge of the reference state from which the pad was tilted. The inclination angle is calculated in the same way as [8] and only uses the information from the 3 outer coils.

The calculated misalignment angles are compared to the applied misalignment angles in Table 2. The angular deviation is a maximum of 0.14° for the predicted mean angles, with a tilt angle of 1 degree, and the standard deviations are low with a maximum of 0.05° in all experiments. The evaluation shows a very precise prediction of the tilt angles with the set angles.

Tab. 2: Angle evaluation for different tilt configurations.

Config.	Angle °	Pred. angle mean $^\circ$	Pred. angle SD $^\circ$	
Plus X	1	1.04	0.02	
$Minus\ X$	1	1.02	0.05	
$Plus\ Y$	1	0.86	0.05	
$Minus\ Y$	1	0.87	0.05	
Plus X	0.5	0.57	0.02	
$\mathbf{Minus}\ X$	0.5	0.45	0.05	
$Plus\ Y$	0.5	0.45	0.04	
$\mathbf{Minus}\ Y$	0.5	0.40	0.02	

4.4 Discussion

To provide context for the results, it is important to note that even in the optically aligned condition, the sensor output exhibits a residual misalignment of up to 0.12° . As shown in Table 2, the calculated angles deviate by approximately 0.14 degrees from the expected values. When compared with the deviation observed in the aligned state, this level of precision demonstrates the system's suitability for implementing control algorithms in robotic applications, particularly for enhancing the accuracy and efficiency of pick-and-place operations.

To determine a reliable predicted tilt angle, it is important to perform the evaluation within the calibrated compression range. This means that the predicted values are only valid up to the maximum compression according to the calibration, as extrapolation can yield false data. For

this reason, the data is capped at the maximum displacement according to the calibration curves, and no prediction is output. To determine the absolute angle, the mean value is specified with sufficient contact for all predictions and only data within the valid calibration range is considered.

5 Conclusion and outlook

This paper introduces a fully automated procedure for a multi-coil, eddy-current-based sensor that can detect small misalignment angles. This procedure is supported by an optical alignment method that enables calibration curves to be recorded. The entire procedure was subsequently validated in an experiment on tilt angles. This allows for precise angle prediction, on the basis of which an auto-adaptive robot control can be realized.

A key characteristic of the presented methodology for calibration is that it is carried out on the fully assembled sensor system, including all components used in the final robotic application namely, the robot adapter, foam layer, conductive reference plane, PCB, and bioinspired adhesive pad. Each of these components introduces inherent variability due to mechanical tolerances, manufacturing imperfections, or manual assembly. Rather than attempting to idealize or isolate each component, the calibration is performed on the complete sensor stack as it is, ensuring that the derived calibration coefficients inherently account for deviations and make the sensor configuration practically deployable.

In the future, instead of using incremental compression, step 2 can be replaced by continuous measurements, in which case the driving speed is used instead of the step width, both procedures are to be considered analogous, and the synchronization of the sensor and distance data is adapted according to the method used.

Further steps will involve using the center coil to obtain more precise angle information and additional surface information from the process sequence. Additionally, the sensor data evaluation will be extended to include phase information to enable alignment prediction and the determination of further process variables.

Acknowledgment: This research was funded by Federal Ministry of Education and Research as part of project No. 01IS21035B ("GecKI") as well as partially funded by a Fraunhofer Internal Program under the Grant No. Attract 025-601314 awarded to S.C.L Fischer.

References

- Eduard Arzt, Stanislav Gorb, and Ralph Spolenak. "From micro to nano contacts in biological attachment devices".
 In: Proceedings of the National Academy of Sciences of the United States of America 100.19 (2003), pp. 10603–10606.
 ISSN: 0027-8424. DOI: 10.1073/pnas.1534701100.
- [2] Eduard Arzt et al. "Functional surface microstructures inspired by nature – From adhesion and wetting principles to sustainable new devices". In: *Progress in Materials Science* 120 (2021), p. 100823. ISSN: 00796425. DOI: 10.1016/j.pmatsci.2021.100823.
- [3] René Hensel, Karsten Moh, and Eduard Arzt. "Engineering Micropatterned Dry Adhesives: From Contact Theory to Handling Applications". In: Advanced Functional Materials 28.28 (2018). ISSN: 1616-301X. DOI: 10.1002/adfm. 201800865.
- [4] Mattia Bacca et al. "Load sharing in bioinspired fibrillar adhesives with backing layer interactions and interfacial misalignment". In: *Journal of the Mechanics and Physics* of Solids 96 (2016), pp. 428–444. ISSN: 0022-5096. DOI: 10.1016/j.jmps.2016.04.008.
- [5] Jamie A. Booth et al. "Benefit of Backing-Layer Compliance in Fibrillar Adhesive Patches—Resistance to Peel Propagation in the Presence of Interfacial Misalignment". In: Advanced Materials Interfaces 5.15 (2018), p. 1800272. ISSN: 2196-7350. DOI: 10.1002/admi.201800272.
- [6] Elmar Kroner et al. "Adhesion of Flat and Structured PDMS Samples to Spherical and Flat Probes: A Comparative Study". In: The Journal of Adhesion 87.5 (2011), pp. 447–465. ISSN: 0021-8464. DOI: 10.1080/00218464. 2011.575317.
- [7] Lena Barnefske et al. "Tuning the Release Force of Microfibrillar Adhesives by Geometric Design". In: Advanced Materials Interfaces 9.33 (2022), p. 2201232. ISSN: 2196-7350. DOI: 10.1002/admi.202201232.
- [8] Simon Herter, Philipp Stopp, and Sarah C.L. Fischer. "Soft Tactile Coil-Based Sensor for Misalignment Detection of Adhesive Fibrillary Gripping Systems". In: Advanced Sensor Research 3.1 (2024). ISSN: 2751-1219. DOI: 10.1002/adsr. 202300098.
- [9] Gregory de Boer et al. "Design Optimisation of a Magnetic Field Based Soft Tactile Sensor: Design Optimisation of a Magnetic Field Based Soft Tactile Sensor". In: Sensors 17.11 (2017), p. 2539. ISSN: 1424-8220. DOI: 10.3390/ s17112539. URL: https://www.mdpi.com/1424-8220/17/ 11/2539.
- [10] Hongbo Wang et al. "Design and Characterization of Tri-Axis Soft Inductive Tactile Sensors". In: IEEE Sensors Journal 18.19 (2018), pp. 7793–7801. ISSN: 1530-437X. DOI: 10.1109/jsen.2018.2845131.
- [11] Hongbo Wang et al. "Robust and high-performance soft inductive tactile sensors based on the Eddy-current effect".
 In: Sensors and Actuators A: Physical 271 (2018), pp. 44–52. ISSN: 0924-4247. DOI: 10.1016/j.sna.2017.12.060.